

technical memorandum

Daresbury Laboratory

DL/SCI/TM92E

SAXS/WAXS EQUIPMENT

by

W.BRAS, G.E.DERBYSHIRE, A.J.RYAN, G.MANT, N.GREAVES, SERC Daresbury Laboratory

FOR
REFERENCE
ONLY

FEBRUARY, 1993

G93/38

DARESBU
RY
LABORATORY
19 FEB 1993
LIBRARY

FOR
REFERENCE
ONLY

Science and Engineering Research Council

DARESBU
RY
LABORATORY

Daresbury, Warrington WA4 4AD

CCLRC LIBRARY & INFO SERVICES



C1005809

© SCIENCE AND ENGINEERING RESEARCH COUNCIL 1993

Enquiries about copyright and reproduction should be addressed to:—
The Librarian, Daresbury Laboratory, Daresbury, Warrington,
WA4 4AD.

ISSN 0144-5677

IMPORTANT

The SERC does not accept any responsibility for loss or damage arising from the use of information contained in any of its reports or in any communication about its tests or investigations.

Report on SAXS/WAXS equipment and experiments performed October 1992.

- 1 Introduction**
- 2 Description of equipment**
- 3 Setting up**
 - 3.1 Beamline**
 - 3.2 Sample environment**
- 4 Electronics and software**
- 5 Performance detectors**
- 6 Some results**
 - 6.1 Spatial resolution**
 - 6.2 q-range**
 - 6.3 Time resolution**
 - 6.4 Polymers**
 - 6.5 Biological samples**
 - 6.6 Further material science**
- 7 Conclusions**

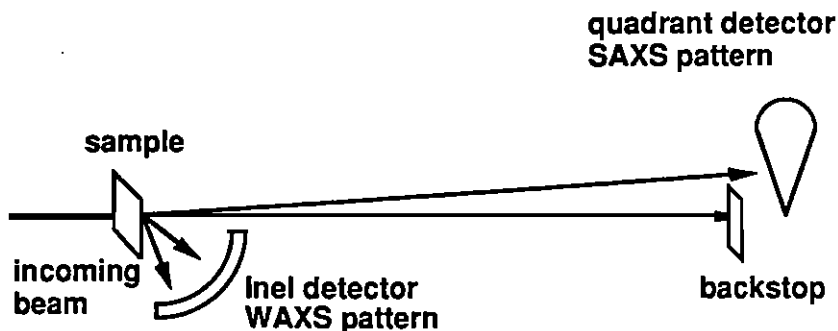
1 Introduction

In this report we will describe our experiences with the set-up for combined time resolved SAXS and WAXS experiments on station 8.2. A description of the set-up will be given as well as an indication where the equipment should be improved in order to bring the system up to the standard of a user facility. Some results, on a variety of samples, will be shown as well.

2 Description of equipment

Compared with the set-up used in the initial experiments, performed in November 1991, three important changes were made. (The initial set-up is described in the Daresbury Annual Report '91/'92).

- A new vacuum vessel was installed in order to overcome the problem with the large air gaps.
- The electronics of the INEL detector were integrated in the data acquisition system of 8.2.
- The INEL detector was mounted so that the scattering pattern below the direct beam could be observed. In theory this means that the data gap could be eliminated completely.



Schematic diagram of the combined SAXS/WAXS experiments

Figure 1

The INEL detector was mounted with the help of MicroControle optical bench parts, providing horizontal, vertical and rotational adjustment. The new vacuum vessel was attached to the standard vacuum chamber. At the sample position a rectangular mica window was used. The window at the detector side was made of Mylar. The whole beam tube was fixed near the sample position with a V-shaped block. Horizontal and vertical adjustment was made possible with the help of studding.

Samples could be mounted either with the help of lab stands or could be

mounted in a sample chamber that could be clamped directly to the the vacuum chamber. This chamber was equipped with a temperature controllable sample holder taken from a Linkam furnace. Provisions have been made to insert a DSC head at a later development stage.

The X-ray beam was focussed at a position half way between the two detectors.

The SAXS system was basically similar to the conventional SAXS set-up.

3 Setting up

3.1 Beamline

Focussing was done with a vacuum chamber that reached to the position halfway between the two detectors. After this the full camera was built up. It proved to be difficult to align the new vacuum chamber properly. The main problem being the crude horizontal/vertical adjustment at the sample position. Correct alignment was obtained with the help of a laser, aligned with green paper on the position of the quadrant detector. A new beam stop had to be glued into the vacuum chamber.

The alignment took approximately 2.5 days.

Necessary improvements :

- Horizontal/vertical adjustment at the sample position with accurate translators.
- Vertical adjustment of the beam stop should be independent of movements of the vacuum chamber.
- A viewing port and a removable fluorescent screen should be installed at the focussing position.

A commercially available laser system (Safesight) would be very useful. A mounting system for the INEL that allows for more accurate repositioning after taking a detector response would be very useful as well.

These improvements can be implemented before the next scheduling period with only limited costs (< £3k) and effort.

3.2 Sample environment

The sample chamber performed satisfactory. Improvements have to be made, however, with the sample mounting and loading. Since the system is modular

new sample chambers can be mounted, that can be tailored to the special requirements of individual users (e.g temperatures outside the range -150° - $+550^{\circ}\text{C}$, fast temperature quenches, high pressures, translating cells).

4 Electronics and software

The integration of the INEL electronics proved to be successful. The full versatility of the NCD data acquisition system could be maintained. The INEL detector memory tended to overload rather quick. This can be overcome by using a memory with one data bit more.

The software worked satisfactory, with only minor problems with the graphics option. A serious problem is the problem of the limited amount of time frames (256), which makes the study of fast processes difficult. In temperature quench experiments the occurrence of phase transitions is not always predictable. In which case 256×0.1 sec frames is not sufficient. The culprit is the Time Frame Generator. This problem will be solved when the new electronics system will be introduced.

5 Performance detectors

The performance of the quadrant detector is well characterised. The only remark is that for most test experiments the detector had to be attenuated by 1 or 2 X-ray films.

As predicted, the INEL proved to be the weak part of the system. In general it had to be attenuated by a factor between 3 till 200 (0.08 - 0.4 mm of Aluminium). With the majority of samples a factor 70 was sufficient. This seriously impairs the possibility of obtaining sub second time resolution.

6 Some results

Several parameters of the system were studied. Some results of test experiments are shown. The major part of the test samples were polymer samples. These were chosen for the simple reason that by adjusting the sample thickness it is easy to vary the count rate. Another advantage is that it is possible to influence the time scale at which phase transitions take place.

6.1 Spatial resolution

Due to the fact that the X-ray beam was focussed between the two detectors some loss of spatial resolution has to be expected. The SAXS data proved to be still of good quality. The WAXS data is compared with results obtained from a conventional diffractometer and is shown to have superior spatial resolution.

In figure 2 the pattern of wet rat tail collagen is shown. Sample-detector distance was set to 4 meter. In figure 3 the pattern, obtained with the INEL detector, of NBS silicon powder diffraction standard number B is shown.

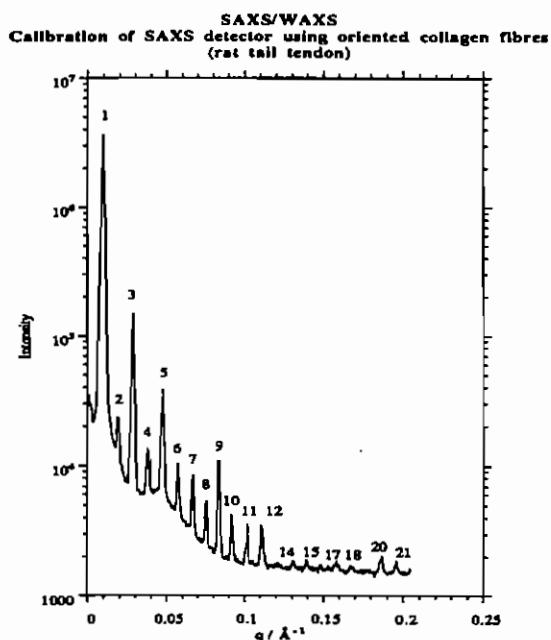


Figure 2

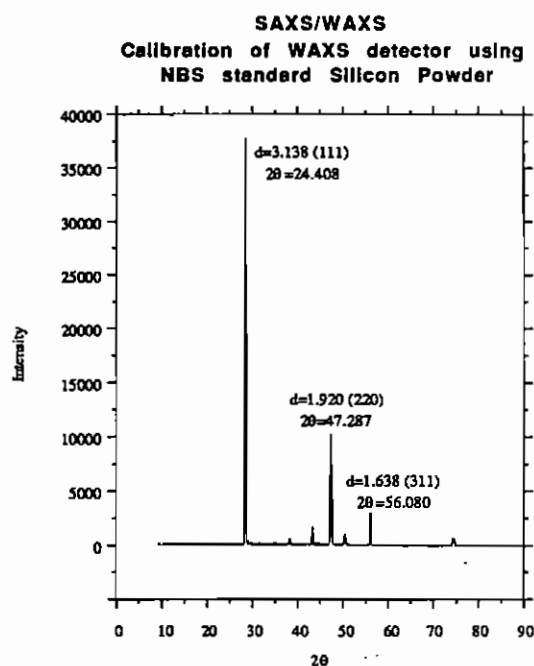


Figure 3

The spatial resolution of the WAXS data proved to be superior to data obtained from conventional diffractometers. Below two examples are given from polymer samples (figure 4a,b). The data is compared with data from a Philips $\theta/2\theta$ diffractometer using filtered Cu $K\alpha$ radiation.

The attention is drawn to HDPE diagram (figure 4b) where it is clear that in the INEL data the peak of the amorphous halo is resolved with respect to the first diffraction peak. This is not seen on the diffractometer data.

The diffractometer scans generally take 40 minutes, the INEL data was collected in 30 seconds.

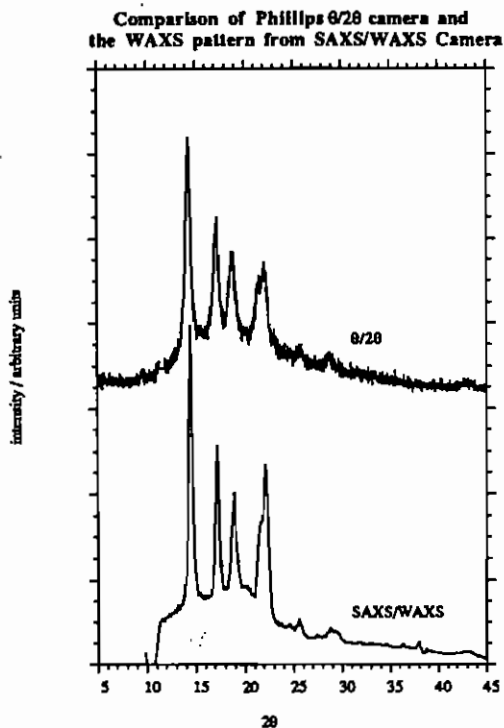


Figure 4a

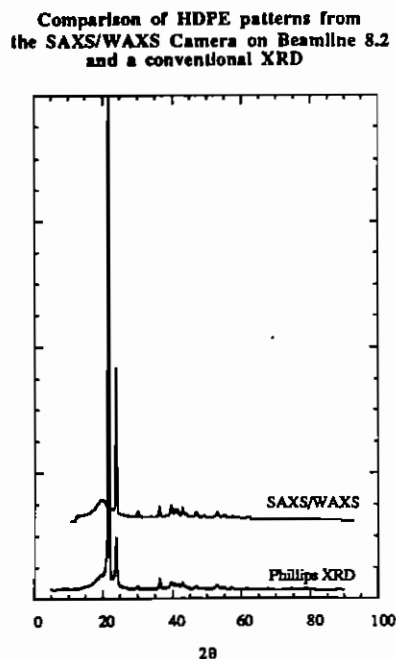


Figure 4b

q-range

Attempts to eliminate the gap in the data range were not undertaken due to the fact that changing the camera length had serious (time consuming) consequences for the alignment of the system. With better adjustment possibilities this will be trivial. The data range obtained with the sample-quadrant distance set to 4 meter and 1 meter between the two last slit sets was :

quadrant :	d: 32 - 800 Å,	q: 0.20 - 0.0079 Å ⁻¹
INEL :	d: 1.1 - 15 Å,	q: 5.7 - 0.41 Å ⁻¹

6.3 Time resolution

The system time resolution is identical to the standard NCD data acquisition system. More interesting is the practical obtainable time resolution, which is a function of the X-ray flux, detection efficiency and the statistical accuracy that the experimenter requires. In figure 5 data derived from a temperature quench

experiment on polyethylene is shown. Quench rate was $10^{\circ}\text{C}/\text{second}$. Time resolution 0.1 sec. The INEL detector was attenuated with 0.16 mm Aluminium. The Quadrant detector with 2 sheets of X-ray film. Ring current 150 mA. Station intensity reduced with horizontal slits to approximately 60%.

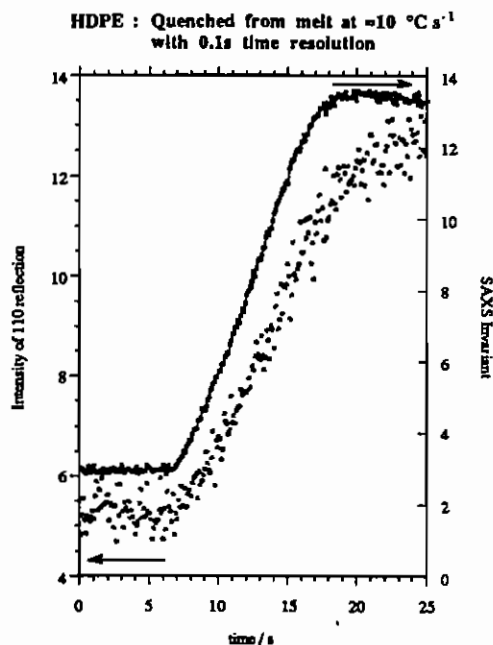


Figure 5
HDPE quenched with $10^{\circ}\text{C}/\text{sec}$ from 150° to 50°C with 0.1 sec time resolution. Invariant derived from SAXS data, the degree of crystallinity from the WAXS data.

The statistics in the curves based upon the WAXS data are rather poor. This proves that the INEL detector is the weak link in the chain. Unfortunately this kind of material is not really suitable for temperature cycling, which would have given the possibility to improve the statistics. Despite this it is possible to obtain physically significant data with a time resolution that mimics industrial processes.

6.4 Polymers

A variety of polymers have been investigated. Among which the well known, commercially interesting materials, High Density Polyethylene (HDPE) and polypropylene. Besides these some newly synthesised liquid crystalline block copolymers have been used. Two examples are shown.

Figures 5 and 6 show diffraction curves obtained from heating/cooling cycles experiments on High Density Polyethylene (HDPE) and on a liquid crystalline block copolymer.

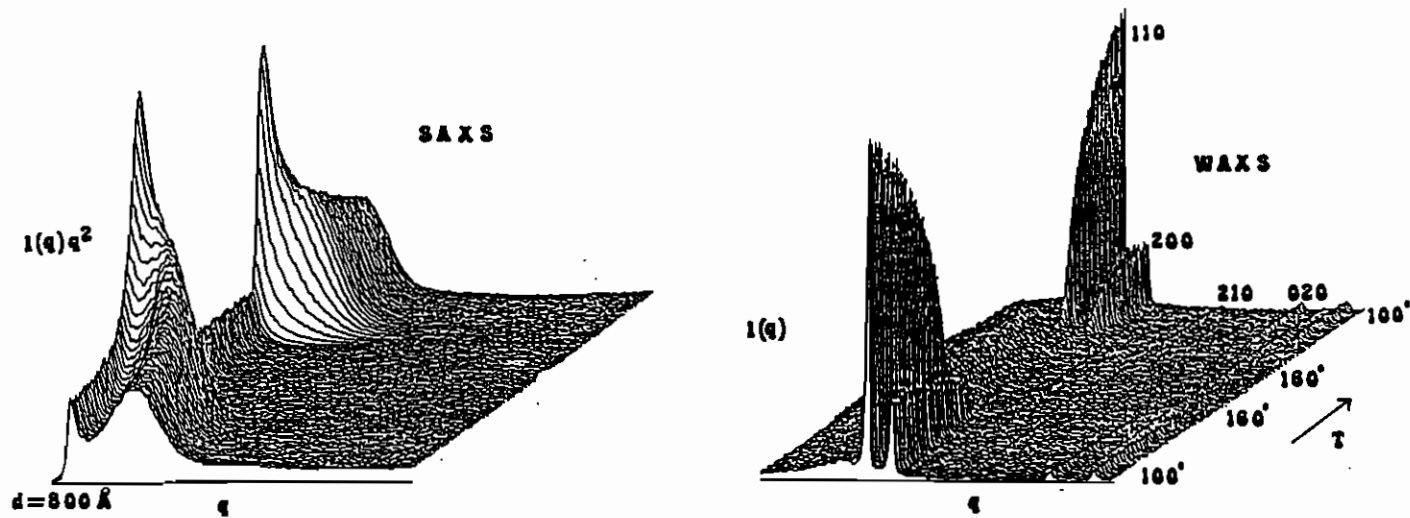


Figure 5
 Temperature cycling experiment on HDPE. Temperature scan rate 6°C/minute. Time resolution 10 seconds/frame. In the SAXS pattern it can be seen that the electron density contrast increases and the distance between the lamellae increases as the melting starts. The phase transitions are clearly reversible.

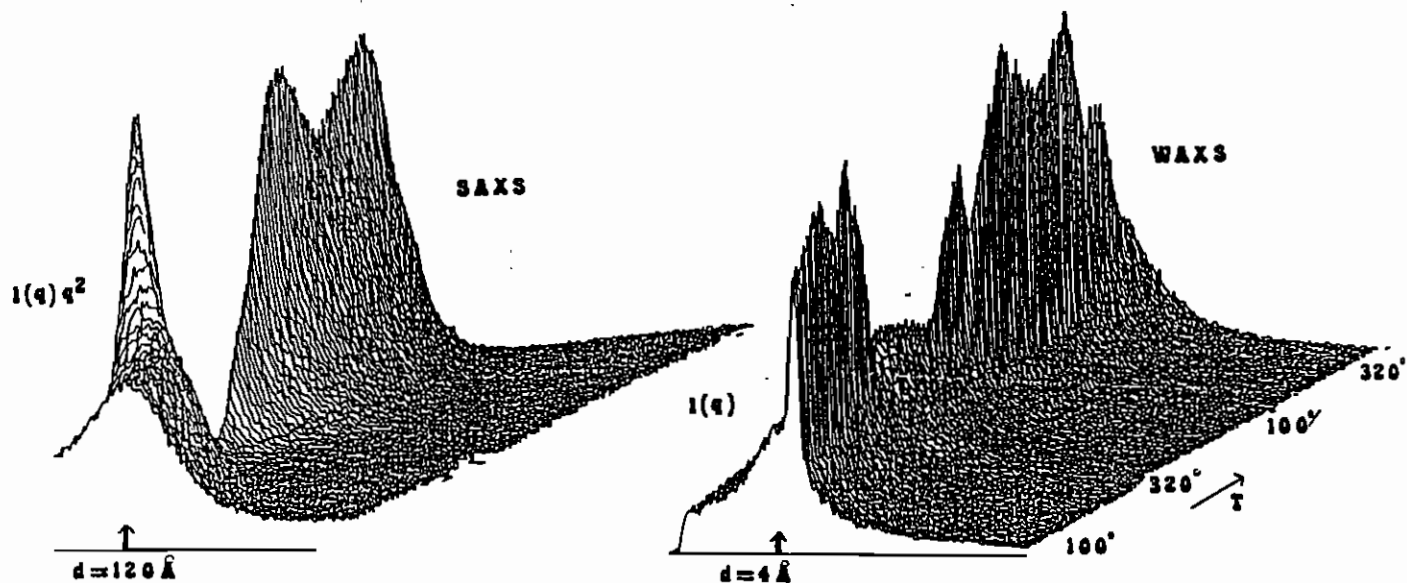


Figure 6
 Temperature scan of liquid crystalline block copolymer. Temperature scan rate 20°C/minute. The SAXS data show an irreversible phase transition from a lamellar block structure to a disordered block structure. The WAXS part shows a reversible crystalline to smectic phase transition.

6.5 Biological

Further test experiments have been performed on bovine corneas. These experiments are normally performed on two different beamlines and generally difficult to interpret due to differences in the degree of hydration caused by the time lag between the two independent experiments. Unfortunately these experiments suffered from the fact that one of the data regions of particular interest was located in the data gap. As mentioned before this problem can be overcome. (samples provided by K.Meek, Open University)

The effect that a slow temperature change has on the lipid structure in human stratum corneum has been investigated. Independent SAXS and WAXS experiments on these samples have been performed but have been proven difficult to interpret due to the limited lifetime of the samples and variations between samples of different donors. (samples provided by J.A.Bouwstra, Leiden University)

6.6 Further material science

In figure 7 the gelatinisation of starch is shown as a function of temperature.

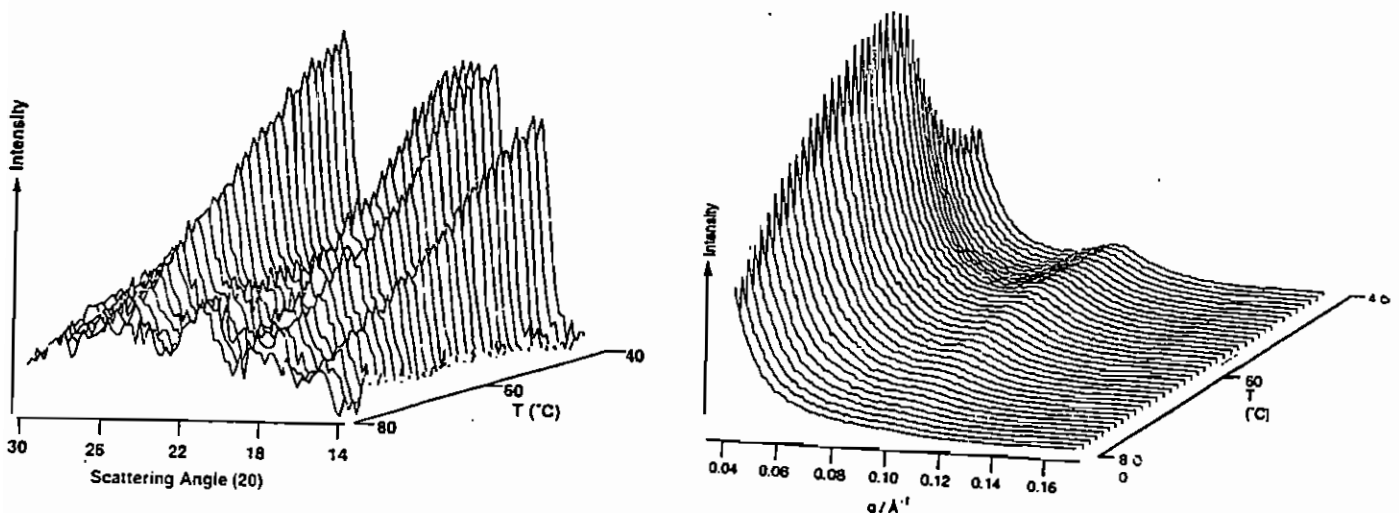


Figure 7

The process of gelatinisation is accompanied by a reduction in intensity for the WAXS peaks. This loss of crystallinity is associated with the dissociation of the amylopectin double helices. Contrary to previous speculation it is shown here that even in the case of limiting water these structural changes occur throughout the entire gelatinisation region (roughly 50° to 80°C). The single peak in the SAXS data exhibits a corresponding loss in intensity, due to the disruption of the lamellar structure as water penetrates the granule. (samples provided by R.Cameron, P.Jenkins, Cavendish Laboratory)

Figure 8 shows the changes that occur when a $Mg_2A_{14}Si_5O_{18}$ corduriete glass sample has been heat treated at 900°C (off-line). The annealing behaviour of this material is not well understood and, although it will be a time consuming experiment, it would be a considerable advantage to study this process on-line, since the sample can be kept continuously at this high temperature.

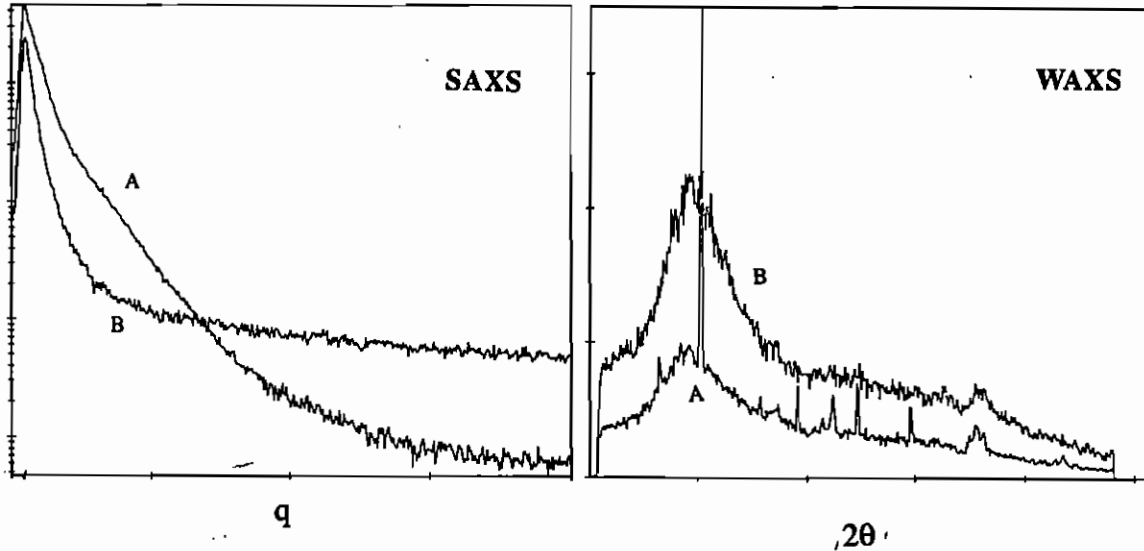


Figure 8

The curves marked B and A represent data before and after heat treatment. In the WAXS region the diffuse scatter decreases and Bragg peaks come up indicating an increase in crystallisation. The SAXS data show that larger order structures are developing as well. (samples provided by M. Oversluizen, S.A Clarke, G.N.Greaves, Daresbury Laboratory, NWO)

Creams were investigated and it was shown that very interesting results can be obtained.(samples provided by E.Towns-Andrews, M.Behan, Daresbury Laboratory)

The study of the structure and freezing process of super cooled water requires a complicated sample environment due to the fact that temperature fluctuations over the sample have to be avoided at all costs. Successful experiments (see figure 9) have been performed showing that it is possible to interface complicated equipment to the SAXS/WAXS set-up. (samples provided by J.Michielsen, J.Dings, J.v.d.Elsken, Amsterdam University)

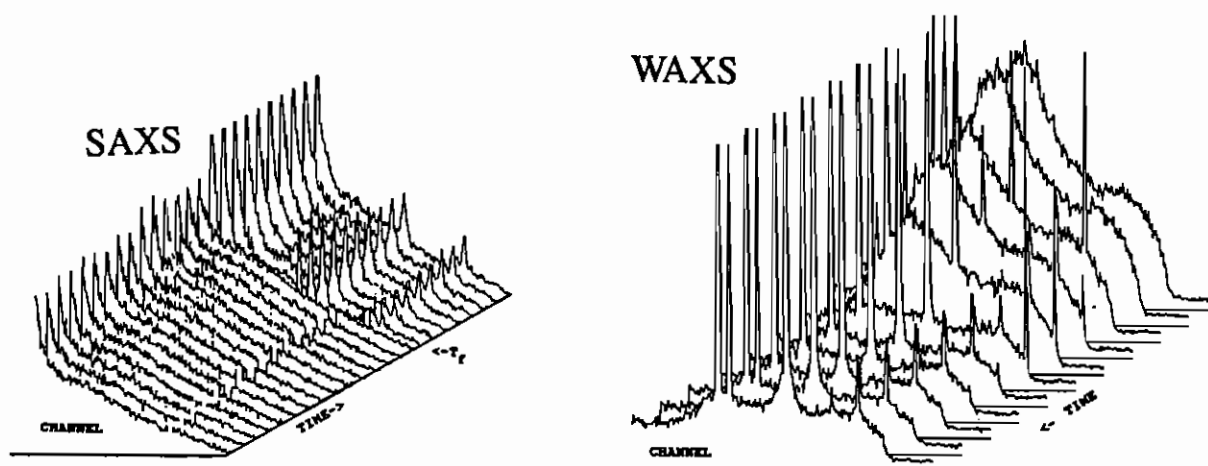


Figure 9

Time resolved data showing the freezing of supercooled water. For clarity the time scales are reversed in the SAXS and WAXS pictures, although both diagrams are obtained simultaneously. Data frame length 20 sec. In the WAXS pattern it is clear that the scattered intensity of water decreases while Bragg reflections due to ice formation appear. In the SAXS spectra superstructure peaks are visible upon freezing, indicating a long range order in the fresh ice.

Phase transformations in artificial membranes are presently studied in Daresbury using a short camera that proves to be difficult to align so that the relevant scattering regions can be observed. The use of a linear detector causes serious smearing on the data towards the higher q -values. In figure 10 a representative data set is shown. The new set-up allows data to be collected over a greatly improved q -range without smearing. The sharp peaks, due to ice formation, around $s = 5\text{nm}^{-1}$ will show up as low noisy 'blobs' when using the old set-up.

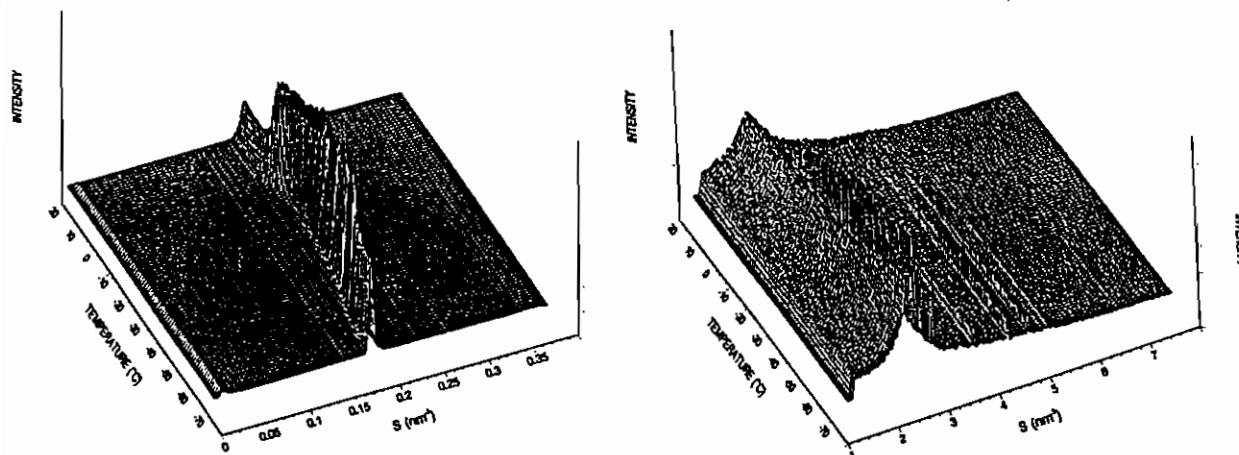


Figure 10

Dilinoleoyl phosphatidylcholine in water undergoing a heating scan of $5^\circ/\text{min}$ from a gel state (at -70°C) to a liquid crystalline state. The lamellar d-spacing

changes when the ice, intercalated in the membrane, starts to melt. This process is of importance for food processing and preservation.

7 Conclusions

We have shown that it is feasible to perform a wide variety of experiments with the equipment described in this report. The data obtained with the help of this set-up produces data that is superior to data obtained at similar set-ups at the Photon Factory, Brookhaven and Hamburg synchrotrons. We have shown some of the results obtained so far but definitely not an exhaustive list. Some of the test experiments have provided sufficient data to justify publication in other than instrumentation journals. The first two manuscripts have been submitted and several others (≈ 6) are being written. Although we know that the first experiments of this kind took place more than 10 years ago we feel that this set-up would be a very useful addition to the experimental facilities at Daresbury.

We would like to thank our colleagues who have made their samples available to us, as well as we would like to thank the technicians and engineers at Daresbury who have made it possible to assemble this set-up.

Wim Bras ¹, Gareth Derbyshire, Tony Ryan, Geoff Mant, Neville Greaves

¹ Wim Bras appears courtesy of the NWO label. Tony Ryan appears courtesy of UMIST records.
Unauthorised copying, public performance, broadcasting, hiring or rental of this report prohibited.